



Photocatalytic Reduction of Methyl Orange, Antibacterial and Anticancer Activities of Biogenic Silver Nanoparticle Synthesized from *Beta vulgaris* Extract

F. FEMINA^{*}, H. ASIA THABASSOOM and J. FELICITA FLORENCE

Department of Chemistry, Holy Cross College (Autonomous), Affiliated to Bharathidasan University, Tiruchirappalli-620002, India

*Corresponding author: E-mail: feminafelix1989@gmail.com

Received: 14 July 2021;

Accepted: 2 September 2021;

Published online: 6 December 2021;

AJC-20591

Studies based on a biogenic synthesis of noble metal nanomaterials has become a promising one in today's biomedical approach in therapy and diagnosis due to multidimensional applications. Hence, the present study is to explore the antibacterial, anticancer and photocatalytic efficacy of silver nanoparticles (AgNPs) synthesized from an extract of *Beta vulgaris* (BV). The band at 398 nm in the UV-visible spectra confirmed the formation of AgNPs. The characteristic shift in OH and C=O peak after the formation of silver nanoparticles shows the participation of *Beta vulgaris* extracts in the reduction process which is further supported by SEM morphology. The average size of the particle (17 nm) was determined from XRD analysis using Scherrer's equation. Antibacterial results of *Beta vulgaris* mediated BV-AgNPs show the maximum zone of inhibition against *Candida albicans*. On anticancer activity, BV-AgNPs reveals the toxicity effect on the MCF-7 cell line with an IC₅₀ value of 40.65 µg/mL. Similarly, it reduces 81.3% of methyl orange at 180 min on the photocatalytic reduction process. This study has suggested an effective replacement for the hazardous chemical methods and leads to a cost-effective, environmentally-friendly method that can also be used as antibacterial and anticancer agents.

Keywords: *Beta vulgaris*, Silver nanoparticles, Antibacterial activity, Anticancer activity, Methyl orange.

INTRODUCTION

In past century, through chemical, physical and greener reduction methods plenty of metal and metal oxide nanoparticles synthesized. Among three methods chemical reduction method is most commonly practiced in large-scale production. However, this method requisite toxic chemicals for the reduction and stabilization process which are unsafe to the environment. Moreover, these toxic chemicals were bounded with final synthesized nanoparticles and it restricts their applications in many fields especially in pharmaceutical fields [1-3].

The plants/plant extracts and microorganisms are the appropriate alternate for chemical and physical reductions, which are non-toxic, reproducible, safe for humans and environment [4]. Microorganism maintenances are time-consuming, expensive and require aseptic conditions also microorganism-based nanoparticles synthesis involves large manual skills and precarious processes on large scale [4-6]. Plants-based greener reduction method is beneficial over microorganism resources and all the parts of plants include bark, fruits, flowers, root,

leaves, stem, rhizoids and latex can be used to synthesize the nanoparticles [7]. Plant extracts contain various medicinally important phytochemicals, which influence to form various dimensions of nanoparticles with the different size and shape which have more effective, applicable, eco-friendly and less toxic than those by physical and chemical procedures [8].

Among all metal and metal oxide nanoparticles in the past few years, silver and gold nanoparticles have prominently focused the scientist's attention due to their applications in numerous fields such as cosmetics, catalytic, plastics, antimicrobial, textile fabrics and drug delivery. Metallic silver or silver nanoparticles get more attention than gold nanoparticles due to their economic, efficiency and has excellent degradation properties on different toxic industrial dyes [7-10].

Present work aimed to synthesize novel and biogenic stable colloidal silver nanoparticles mediated by ecofriendly reducing agent *Beta vulgaris* extract. *Beta vulgaris* (Beet root) extract commonly known as beet greens and belongs to the family Amaranthaceae. *Beta vulgaris* consists of numerous pharmacologically active phytochemicals including the betalains like

β -xanthins and β -cyanins followed by polyphenolics, flavonoids, in addition to inorganic nitrates and rich sources of micro and macrominerals were reported [11,12]. Betanin so-called beet root red is the most common pigment in beet roots is responsible for their strong colour. As a nutritious rich source, the beetroot holds the pharmacological actions such as antioxidant, anti-inflammatory effects, anticarcinogenic, antimicrobial, anti-diabetic, antibacterial and wound healing properties [11-14].

Since *Beta vulgaris* extract is used as a reducing agent which can enhance the potential of AgNPs. Bioactive organic compounds in the *Beta vulgaris* extract may form complex with silver and reduces the silver ions into silver nanoparticles. This greener reduction process controls the production of toxic AgNPs and hazardous byproducts. Present work aimed to synthesis the ecofriendly *Beta vulgaris* mediated AgNPs and their characterizations by UV-vis, FT-IR, SEM, XRD, EDAX and zeta potential. Furthermore, the antibacterial, anticancer and photocatalytic degradation of methyl orange dye were investigated on synthesized *Beta vulgaris* mediated AgNPs.

EXPERIMENTAL

Preparation of *Beta vulgaris* extract: *Beta vulgaris* was washed several times with water to remove dust particles. Cleaned *Beta vulgaris* (250 g) were chopped into fine pieces and transfer into a 500 mL beaker. Then, double distilled water was added and boiled at 50 °C at 60 min until the colour of the aqueous solution turned into deep red colour. The obtained extract was cooled and then filtered using normal paper followed by Whatman No. 1 filter paper. The final filtrate was stored in a refrigerator for further qualitative analysis and nanoparticle synthesis.

Preparation of green silver nanoparticles: For green AgNPs synthesis, 50 mL *Beta vulgaris* extract and 50 mL of 0.01 M silver nitrate solution were used. Initially, 50 mL silver nitrate solution was taken in a 500 mL beaker to this, 10 mL *Beta vulgaris* extract was added then stirred well on the magnetic stirrer for 1 h. Every 1 h interval, 10 mL of *Beta vulgaris* extract was added (5 additions). After that, the final deposited particles were collected by centrifugation at 6000 rpm and washed with double distilled water followed by heating in a hot air furnace at 150 °C for 18 h. The obtained brown powder was ground into a fine powder using a mortar and pestle then, took for characterization and other pharmacological applications [15,16].

Characterization of green AgNPs: Synthesized *Beta vulgaris* mediated AgNPs were characterized by UV-visible spectrometer, FTIR, SEM, XRD and EDX. FT-IR helped to identify the probable functional groups which are involved in the reduction of Ag^+ to Ag^0 . FT-IR analysis observed from the dried *Beta vulgaris* mediated AgNPs was recorded using KBr. For SEM analysis, a small amount of fine powder of *Beta vulgaris* mediated AgNPs was prepared as thin film and placed on mold by using carbon-coated tape. The surface morphology and quality of silver nanoparticles were investigated by the XRD, the fine powered *Beta vulgaris* mediated AgNPs were analyzed by XRD and the data was collected at 2θ from 5° to 90°. EDX helped to probe the composition of solid materials and to determine the chemical purity as well as elemental

composition, density of the material, stoichiometry and can be used to estimate their relative abundance. The zeta potential of synthesized nanoparticles was studied which commonly determines the surface charge of nanoparticles in solution also predicts the stability of colloidal silver nanoparticles [17-19].

Antibacterial activity: *Beta vulgaris* mediated AgNPs were tested against the antibacterial and antifungal activity as per the Clinical Laboratory Standards Institute guidelines (CLSI). The bacterial activity of *Beta vulgaris* mediated AgNPs was screened by disc diffusion method against *Staphylococcus aureus*, *Bacillus subtilis*, *Pseudomonas aeruginosa*, *Escherichia coli*, *Aspergillus niger* and *Candida albicans*. The nutrient agar medium was prepared and sterilized by autoclaving at 121 °C 15 lbs pressure for 15 min then aseptically poured the medium into the sterile Petri plates and allowed to solidify the bacterial broth culture, then swabbed on each Petri plate using sterile buds. In each plate five wells were made by a well cutter then 50 μL of *Beta vulgaris* extract, silver nitrate solution, gentamicin, double distilled water and silver nanoparticles were poured into each well aseptically. Then the Petri plates were incubated at 37 °C for 24 h. After the incubation period, the plates were taken out and measures the zone of inhibitions [20].

Anticancer activity: MCF-7 cells were trypsinized in 96 well plates, which contain the density of 4000 cells/well in 100 μL and incubated for 24 h. Then 0.1% of 2X concentration of stock solution prepared in the DMEM medium influenced with 10% FCS added (2000, 600, 200, 60, 20, 6 $\mu\text{g}/\text{mL}$) kept in incubation for 2 days to achieve the final concentration 1000, 300, 100, 30, 10 and 3 $\mu\text{g}/\text{mL}$. After incubation, the medium was washed with phosphate solution. After washing, it was placed in a new medium MTT solution composed of 3-(4,5-dimethylthiazol-2-yl)-2,5-diphenyl tetrazolium bromide (MTT) at 5 mg/mL in 1X PBS, Which was incubated for 4 h. After the incubation time, 1mL of DMSO was added and the total viable cells were determined by measuring the absorbance at 540 nm by a microplate reader. From the optical density/absorbance values the percentage of growths or cell viability was calculated by the following formula [21]:

$$\text{Growth (\%)} = 100 \times \frac{(T - T_0)}{(C - T_0)}$$

where, T = optical density of test, C = optical density of control, T_0 = optical density at zero time.

Photocatalytic reduction of methyl orange dye: The investigation was performed in a Heber multi-lamp photo-reactor with a low pressure of 125 W UV lamps (254 nm) under continuous stirring conditions. Photocatalytic behaviour of the *Beta vulgaris* mediated AgNPs in the reduction of methyl orange dye was evaluated after every 30 min interval by taking 3 mL of test sample (methylene orange of 10 ppm) treated with 0.01 g of respective nanomaterial placed on under halogen light source. The reaction progress was noted by recording its absorbance using a UV-visible spectrophotometer. The percentage removal was calculated with the help of standard calibration curve obtained by measuring the absorbance of untreated methylene orange using the following formula [22]:

$$\text{Methylene blue degraded (\%)} = \frac{\text{I.C} - \text{F.C}}{\text{I.C}} \times 100$$

where I.C = initial absorbance of methylene blue (blank); F.C = sample absorbance.

RESULTS AND DISCUSSION

UV-visible studies: After the addition of dark red colloidal solution of *Beta vulgaris* extract into the colourless silver nitrate solution turned into brown, which strongly affirms the formation of *Beta vulgaris* mediated AgNPs in the aqueous medium. Colour changes of the reaction mixture were varied from pale brown to brown than brown to deep brown with respect to the addition of *Beta vulgaris* extracts. The increase of *Beta vulgaris* extract increases the reduction rate of Ag^+ to Ag^0 . UV-visible absorption spectra of *Beta vulgaris* mediated AgNPs show a characteristic absorption peak at 398 nm, which is due to strong and single surface plasmon resonance (SPR) (Fig. 1) [23].

FT-IR studies: FT-IR spectrum (Fig. 2) confirmed the involvement of *Beta vulgaris* extract constituents in the AgNPs synthesis. In the biosynthesized silver nanoparticles the peaks observed at 3426, 2925, 1601, 1383, 1269, 1062, 776 cm^{-1}

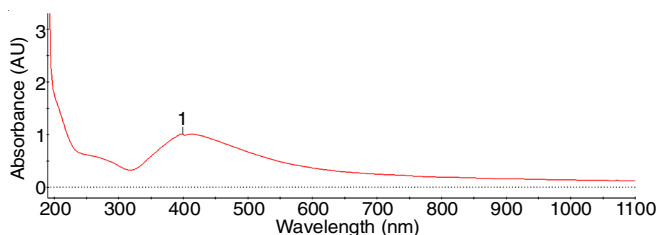


Fig. 1. UV-Visible spectra of BV-AgNPs

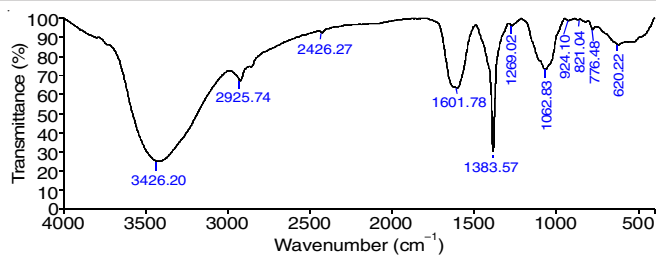


Fig. 2. FT-IR of BV-AgNPs

are associated with O-H stretching, C-H stretching, C=C stretching of a methyl group, O-H bending, C-O stretching and C-H bending, respectively. The range below 650 cm^{-1} is responsible for metal-oxygen bond in *Beta vulgaris* mediated AgNPs.

XRD studies: The XRD analysis (Fig. 3) confirmed the crystallinity nature of *Beta vulgaris* mediated AgNPs based on the emission peaks of 2θ at 38.38° , 44.58° , 64.73° and 77.63° , corresponding to the silver crystal planes (111), (200), (220) and (311), respectively which are in good agreement with the

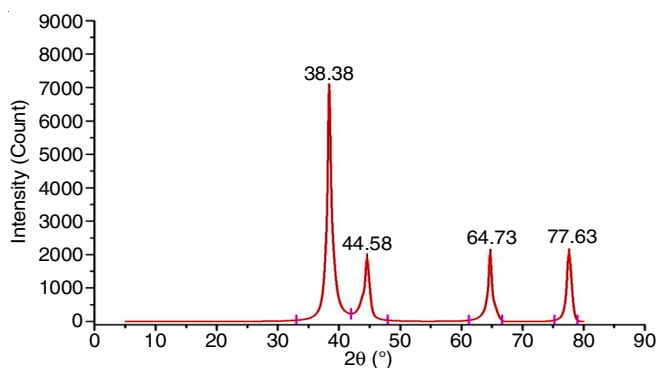


Fig. 3. XRD pattern of BV-AgNPs

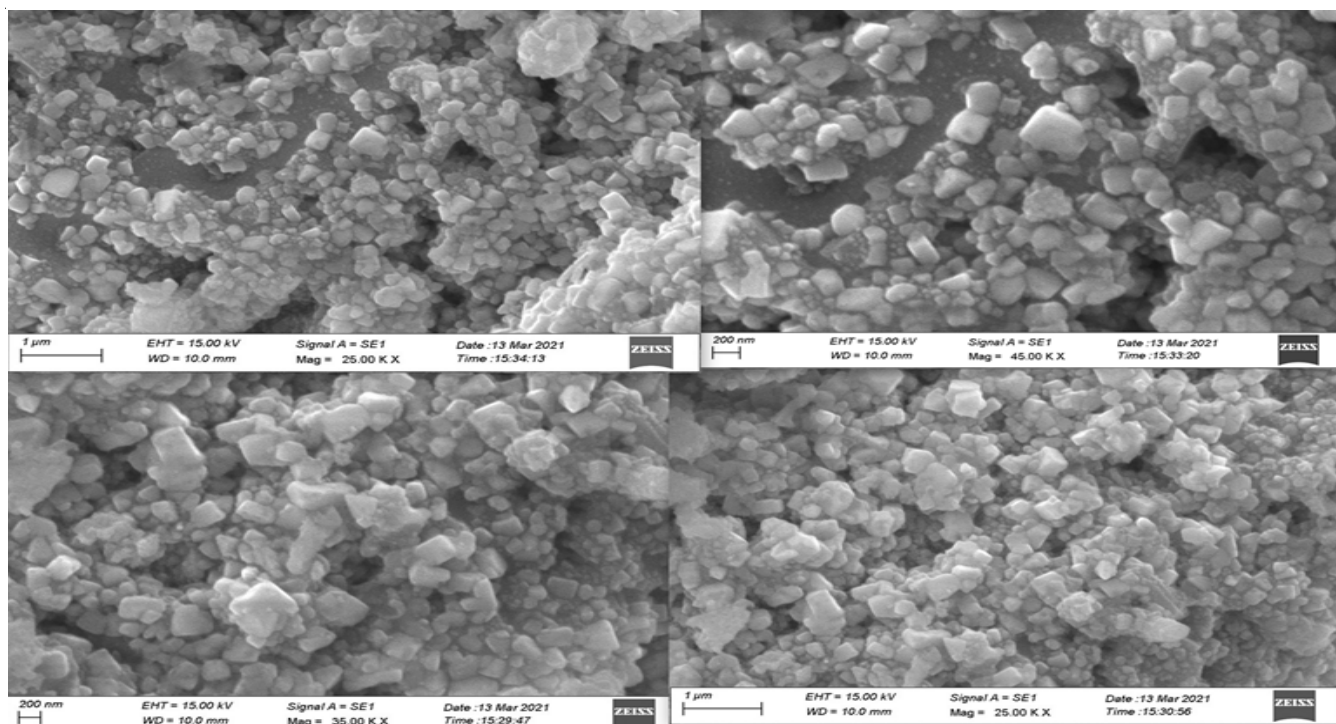


Fig. 4. SEM images of BV-AgNPs

literature report (JCPDS file no. 04-0783). The average grain size of the synthesized material was determined from the FWHM of the XRD peaks using the Scherrer's equation and found to be 17 nm [24].

SEM studies: Different magnification ranges of AgNPs from 1 μm -200 nm *Beta vulgaris* mediated AgNPs are shown in Fig. 4, which shows the polydispersed structure. In SEM micrograph, it was observed that the rectangular, hexagonal and cubic types of silver nanoparticles were formed with the size ranging from 10 to 50 nm. In the greener method, most commonly spherical shapes of AgNPs were reported but in the present case, *Beta vulgaris* mediated AgNPs are in different shapes, which is due to the shape-controlled effect of *Beta vulgaris* extract.

The synthesized AgNPs were subjected to an EDAX spectrum to quantify the mixture of metal and oxides present in the sample. The results (Fig. 5) showed that 69% of silver (Ag), 23% of carbon (C) and 8% of oxygen (O) were present in the resulted *Beta vulgaris* mediated AgNPs. EDAX showed the high intense peak of Ag and the low intense peak of carbon and oxygen were due to the capping actions of biomolecules in the extract.

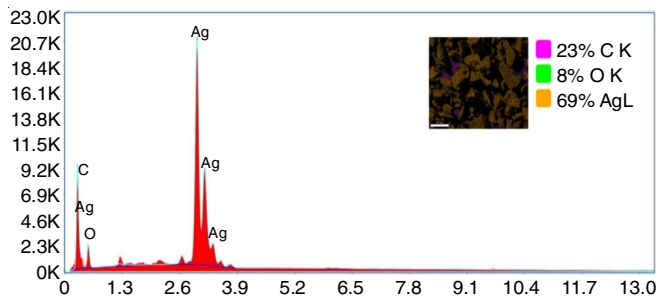
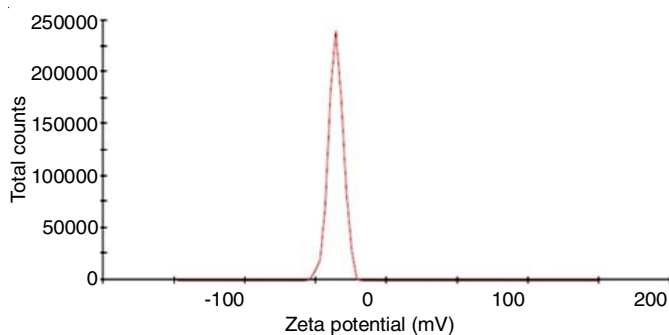


Fig. 5. EDAX of BV-AgNPs



The particle size distribution of *Beta vulgaris* mediated AgNPs is shown in Fig. 6 which showed the various sizes of nanoparticles ranging from 3.033 to 398.6 nm and had an average particle size of 401.6 nm. Precisely, 67.7% of total particles had the size of 398.6 nm and 32.3% had 3.033 nm. Moreover, the difference between the largest and the smallest size of the nanoparticles was 395.6 nm, which indicated the broad distribution of AgNPs. In addition, the zeta potential value was determined as -35.7 mV. The negative value indicated the stability of silver nanoparticles and it evaded the agglomeration of silver nanoparticles. The negative potential value might be due to the capping action of biomolecules present in the *Beta vulgaris* extract [25].

Antibacterial activity of *B. vulgaris* mediated AgNPs: Synthesized *Beta vulgaris* mediated AgNPs were tested against the five pathogens and it showed a well inhibitory effect compared with silver solution, *Beta vulgaris* plant extract and standard antibiotics gentamicin. Maximum zone of inhibition was observed against the *Candida albicans* (30 ± 2.58 mm) followed by *Bacillus subtilis* (26 ± 2.06 mm) while least activity was seen against *Pseudomonas aeruginosa* and *A. niger* (Table-1). Different mechanism of action of nanoparticle against bacteria has been reported in previous literature because of difference in structural composition. The zone of inhibition obtained using *Beta vulgaris* mediated AgNPs was much lower than the standard disc gentamicin used, which depicts the need for further engineering of nanoparticles to obtain desirable effects.

Antibreast cancer activity: Anticancer activity of *Beta vulgaris* mediated AgNPs nanoparticles results shows the exposure of MCF-7 cells to AgNPs nanoparticles at the various concentration for 72 h, significantly that reduce the cell viability in a concentration-dependent manner (Figs. 7-9). As the concen-

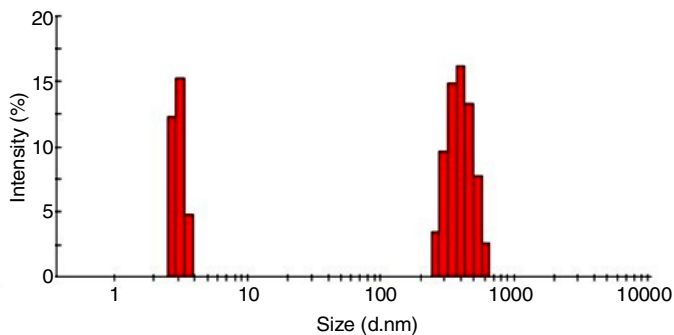


Fig. 6. Particle size analysis of BV-AgNPs

TABLE-1
ANTIBACTERIAL ACTIVITY RESULTS OF *Beta vulgaris* MEDIATED AgNPs

Microorganisms	Zone of inhibition (mm) (50 μL)				
	Negative control (Gentamicin)	Silver nitrate	<i>Beta vulgaris</i> extract	AgNPs	Negative control (water)
<i>Bacillus subtilis</i>	20 ± 1.33	18 ± 1.02	18 ± 1.13	26 ± 2.06	0
<i>Staphylococcus aureus</i>	20 ± 1.16	20 ± 0.81	18 ± 1.01	25 ± 1.33	0
<i>E. coli</i>	20 ± 0.98	20 ± 1.21	20 ± 2.01	25 ± 1.67	0
<i>Pseudomonas aeruginosa</i>	20 ± 3.01	20 ± 1.11	18 ± 1.72	24 ± 3.01	0
<i>Candida albicans</i>	20 ± 2.14	27 ± 2.06	18 ± 2.15	30 ± 2.58	0
<i>A. niger</i>	20 ± 1.52	20 ± 1.86	18 ± 1.23	24 ± 1.56	0

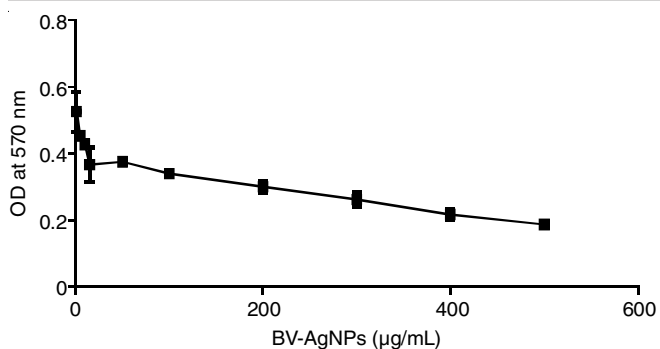


Fig. 7. Concentration vs. absorption graph of BV-AgNPs on MCF-7 cell line

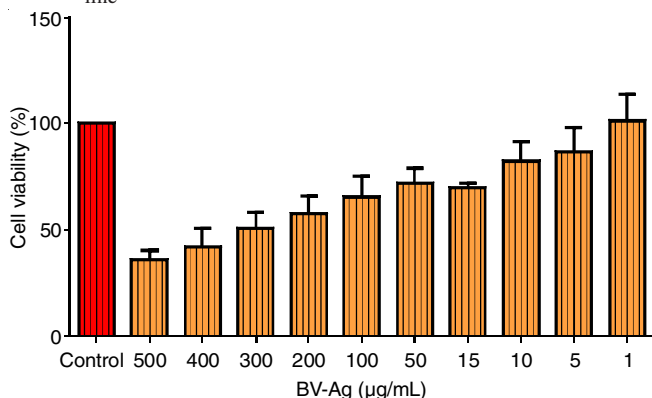


Fig. 8. Concentration vs. cell viability graph of BV-AgNPs on MCF-7 cell line

tration increases the cell viability decreases. For the synthesized BV-AgNPs nanoparticles at 1-500 µg/mL concentrations the absorbance was decreased from 0.526 to 0.187 on MCF-7 cells. For cell viability percentage *Beta vulgaris* mediated AgNPs

decreases the cell viability from 101.18% to 35.91% while increasing the nanoparticle concentrations. Moreover, it shows significant inhibitory and toxic effects on human breast cancer cells with an IC_{50} value of 40.65 µg/mL. The cytotoxicity effect of silver nanoparticles depends on its size and shape because nanoparticles in the 100-160 nm range can directly contact the MCF-7 cell surfaces and initiate the cytotoxicity effects. Folkman's hypothesis states that the formation of new blood vessels promotes the growth of solid tumors in the human body by supplying oxygen and nutrients. Green synthesized AgNPs inhibit the growth of vascular endothelial cells (protective barrier of blood vessels) and blocks blood vessel formation (angiogenesis property). Anti-angiogenesis drugs plays the important role in cancer treatments and these biogenic silver nanoparticles act as angiogenesis inhibitors [26].

AgNPs have boundless applications in the reduction of industrial organic dyes as well as the degradation of toxic dyes and heavy metals. Untreated and *B. vulgaris* mediated AgNPs treated methyl orange dye UV-visible spectral absorption results are shown in Fig. 10. Before adding *B. vulgaris* mediated AgNPs, methyl orange solution exhibits the maximum absorbance, while adding *B. vulgaris* mediated AgNPs the absorbance gets lowered when time extended the degradation percentage increased. At 180 min *B. vulgaris* mediated AgNPs reduced 81.3% of methyl orange solution (Table-2).

Conclusion

The development of the reliable and eco-friendly process is the complex urge in the field of nanotechnology to synthesize metallic nanoparticles. The current study proclaimed that silver nanoparticles can be synthesized by green approaches using *Beta vulgaris*. Because of owing antibacterial and anticancer activities, *B.*

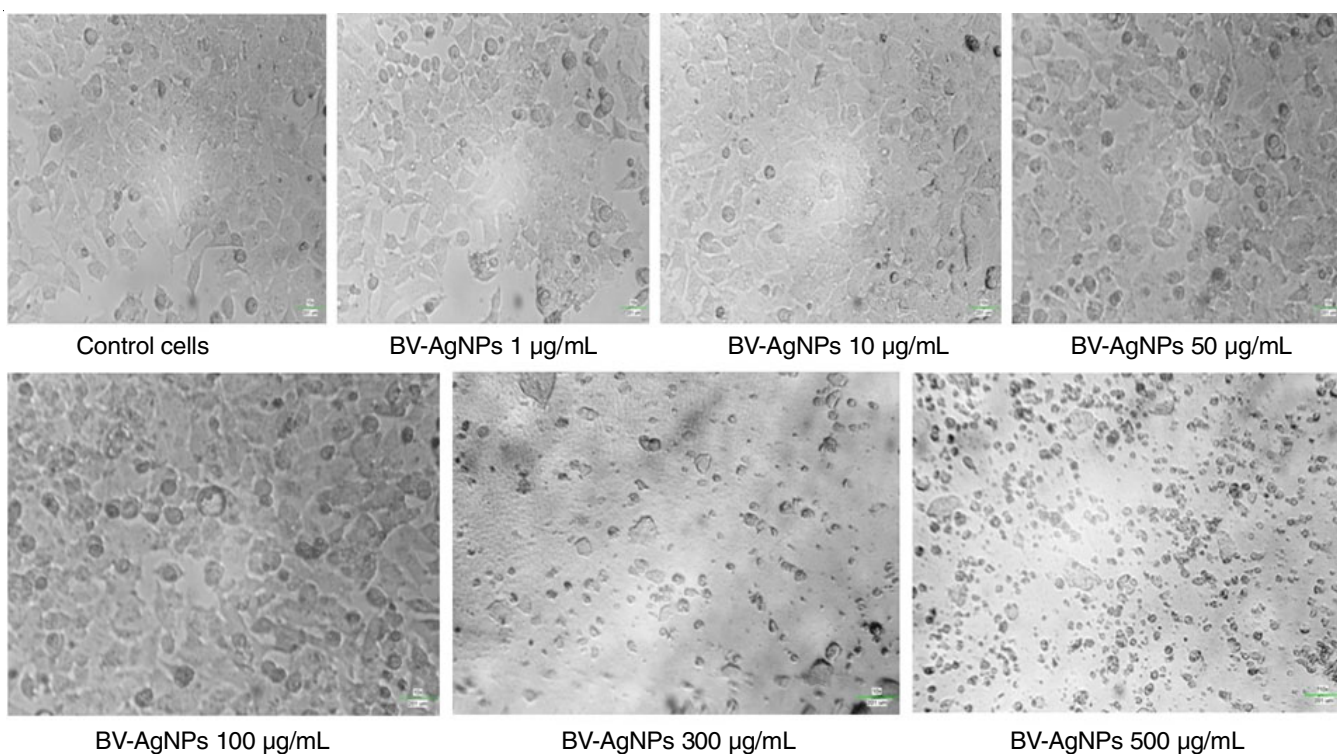


Fig. 9. Antibreast cancer activity images of BV-AgNPs on MCF-7 cell line

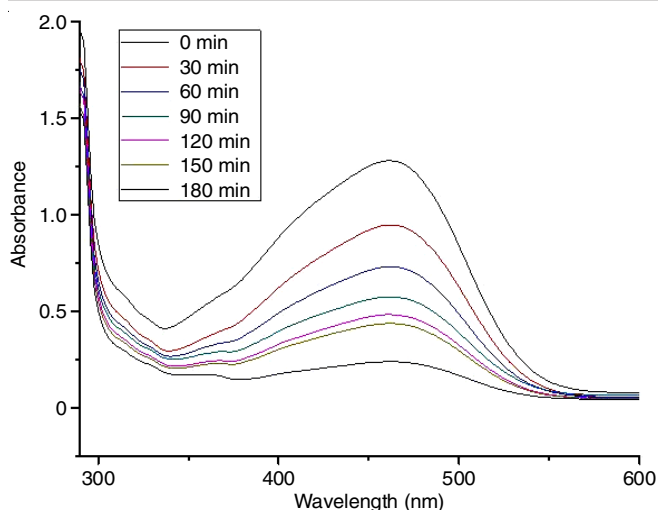


Fig. 10. Photocatalytic degradation of methyl orange on BV-AgNPs

TABLE-2
PHOTOCATALYTIC DEGRADATION
OF METHYL ORANGE ON BV-AgNPs

Time (min)	Initial absorbance (Blank)	Sample absorbance	Percentage of degradation
0	1.279	1.279	0
30	1.279	0.947	25.95778
60	1.279	0.731	42.84597
90	1.279	0.574	55.12119
120	1.279	0.483	62.23612
150	1.279	0.437	65.83268
180	1.279	0.239	81.31353

vulgaris mediated AgNPs can be used in pharmaceuticals. Owing to its catalytic activity, *B. vulgaris* mediated AgNPs may be applicable in the dye and paint industries for wastewater treatments. Thus, this study had the potential value to develop new silver nanoparticles with better activity and help in the biocontrol of diseases.

CONFLICT OF INTEREST

The authors declare that there is no conflict of interests regarding the publication of this article.

REFERENCES

- M. Vanaja, K. Paulkumar, M. Baburaja, S. Rajeshkumar, G. Gnanajobitha, C. Malarkodi, M. Sivakavinesan and G. Annadurai, *Bioinorg. Chem. Appl.*, **2014**, 742346 (2014); <https://doi.org/10.1155/2014/742346>
- P. Logeswari, S. Silambarasan and J. Abraham, *J. Saudi Chem. Soc.*, **19**, 311 (2015); <https://doi.org/10.1016/j.jscs.2012.04.007>
- K. Chand, D. Cao, D. Eldin Fouad, A. Hussain Shah, A. Qadeer Dayo, K. Zhu, M. Nazim Lakhan, G. Mehdi and S. Dong, *Arab. J. Chem.*, **13**, 8248 (2020); <https://doi.org/10.1016/j.arabjc.2020.01.009>
- R. Jacoby, M. Peukert, A. Succurro, A. Koprivova and S. Kopriva, *Front. Plant Sci.*, **8**, 1617 (2017); <https://doi.org/10.3389/fpls.2017.01617>
- A.E.M. Dalia and E.M. Taher, *J. Phys. Conf. Ser.*, **1294**, 062048 (2019); <https://doi.org/10.1088/1742-6596/1294/6/062048>
- I.X. Yin, J. Zhang, I.S. Zhao, M.L. Mei, Q. Li and C.H. Chu, *Int. J. Nanomedicine*, **15**, 2555 (2020); <https://doi.org/10.2147/IJN.S246764>
- S. Satpathy, A. Patra, B. Ahirwar and M.D. Hussain, *Artif. Cells Nanomed. Biotechnol.*, **46**, 72 (2018); <https://doi.org/10.1080/21691401.2018.1489265>
- R. Geetha, T. Ashokkumar, S. Tamilselvan, K. Govindaraju, M. Sadiq and G. Singaravelu, *Cancer Nanotechnol.*, **4**, 91 (2013); <https://doi.org/10.1007/s12645-013-0040-9>
- Z.A. Ratan, M.F. Haidere, M. Nurunnabi, S.M. Shahriar, A.J.S. Ahammad, Y.Y. Shim, M.J.T. Reaney and J.Y. Cho, *Cancers*, **12**, 855 (2020); <https://doi.org/10.3390/cancers12040855>
- K. Venugopal, H. Ahmad, E. Manikandan, K. Thanigai Arul, K. Kavitha, M.K. Moodley, K. Rajagopal, R. Balabhaskar and M. Bhaskar, *J. Photochem. Photobiol. B*, **173**, 99 (2017); <https://doi.org/10.1016/j.jphotobiol.2017.05.031>
- L. Ceclu and O.-V. Nistor, *J. Nutri. Med. Diet Care*, **6**, 43 (2020); <https://doi.org/10.23937/2572-3278.1510043>
- P. Neha, S.K. Jain, N.K. Jain, H.K. Jain and H.K. Mittal, *Int. J. Chem. Sci.*, **6**, 3190 (2018).
- V.G. Georgiev, J. Weber, E.M. Kneschke, P.N. Denev, T. Bley and A.I. Pavlov, *Plant Foods Hum. Nutr.*, **65**, 105 (2010); <https://doi.org/10.1007/s11130-010-0156-6>
- T. Clifford, G. Howatson, D. West and E. Stevenson, *Nutrients*, **7**, 2801 (2015); <https://doi.org/10.3390/nu7042801>
- A.R. Allafchian, S.Z. Mirahmadi-Zare, S.A.H. Jalali, S.S. Hashemi and M.R. Vahabi, *J. Nanostruct. Chem.*, **6**, 129 (2016); <https://doi.org/10.1007/s40097-016-0187-0>
- J.R. Vimala, S.M. Sheela, G.D. Jeyaleela and S.I. Monisha, *World J. Pharm. Res.*, **5**, 998 (2016).
- K.M.M. Abou El-Nour, A. Eftaiha, A. Al-Warthan and R.A.A. Ammar, *Arab. J. Chem.*, **3**, 135 (2010); <https://doi.org/10.1016/j.arabjc.2010.04.008>
- G. Ganapathy Selvam and K. Sivakumar, *Appl. Nanosci.*, **5**, 617 (2015); <https://doi.org/10.1007/s13204-014-0356-8>
- J. Kadam, P. Dhawal, S. Barve and S. Kakodkar, *SN Appl. Sci.*, **2**, 738 (2020); <https://doi.org/10.1007/s42452-020-2543-4>
- M. Gomathi, A. Prakasam, P.V. Rajkumar, S. Rajeshkumar, R. Chandrasekaran and P.M. Anbarasan, *S. Afr. J. Chem. Eng.*, **32**, 1 (2020); <https://doi.org/10.1016/j.sajce.2019.11.005>
- R. Khateef, H. Khadri, A. Almatroudi, S.A. Alsuhaibani, S.A. Mobein and R.A. Khan, *Adv. Nat. Sci.: Nanosci. Nanotechnol.*, **10**, 045012 (2019); <https://doi.org/10.1088/2043-6254/ab47ff>
- M. Li, R. Guan, J. Li, Z. Zhao, J. Zhang, Y. Qi, H. Zhai and L. Wang, *ACS Omega*, **5**, 21455 (2020); <https://doi.org/10.1021/acsomega.0c01832>
- S. Raja, V. Ramesh and V. Thivaharan, *Arab. J. Chem.*, **10**, 253 (2017); <https://doi.org/10.1016/j.arabjc.2015.06.023>
- E. Yuksel, Y.E. Taskesen, D. Erarslan and R. Canhilal, *Egypt. J. Biol. Pest Control*, **28**, 8 (2018); <https://doi.org/10.1186/s41938-017-0019-7>
- M.J. Haider and M.S. Mehdi, *J. Sci. Eng. Res.*, **5**, 385 (2014);
- B. Venkatadri, E. Shanparvish, M.R. Rameshkumar, M.V. Arasu, N.A. Al-Dhabi, V.K. Ponnusamy and P. Agastian, *Saudi J. Biol. Sci.*, **27**, 2980 (2020); <https://doi.org/10.1016/j.sjbs.2020.09.021>